ELSEVIER

Polymer Vol. 37 No. 10, pp. 1787–1795, 1996

0032-3861/96/$15.00 + 0.00

Molecular dynamics computer simulation of local dynamics in polyisoprene melts

Neil E. Moe and M. D. Ediger*
Department of Chemistry, University of Wisconsin, 1101 University Avenue, Madison, WI 53706, USA
(Received 15 May 1995; revised 19 June 1995)

Fully atomistic molecular dynamics computer simulations of *cis*-polyisoprene melts have been performed. Two different methods were used to generate four initial configurations. The local polymer dynamics were substantially independent of initial chain configuration. The ratios of correlation times for different C–H vectors in the chain backbone match experiment very well. Absolute correlation times from the simulation are about 2.5 times slower than experimental values. The correlation functions obtained from the simulations are strongly non-exponential, in general agreement with experiment. The local dynamics in these simulations are fairly isotropic, in marked contrast to results reported from simulations of polyethylene melts by Takeuchi and Roe. Several analysis techniques indicate that the spatial extent of the cooperative motion that accompanies conformational transitions in polyisoprene melts is about 1–2 repeat units. A similar length scale was found recently in simulations of polyisoprene in a dilute solution. Copyright © 1996 Elsevier Science Ltd.

(Keywords: local dynamics; conformational transitions; polyisoprene melts)

INTRODUCTION

The local dynamics of polymers play an important role in determining macroscopic properties such as the glass transition temperature T_g and the temperature dependence of the viscosity. As the temperature is lowered through T_g, the shear modulus typically increases by three orders of magnitude as molecular motions become slow compared to the experimental timescale (e.g. ref. 1). Since T_g is independent of molecular weight at high molecular weight, the motions responsible for this dramatic change cannot involve the entire chain. Experiments indicate that very local dynamics, of the order of a few repeat units, determine T_g (refs 2, 3).

Molecular dynamics computer simulations have been increasingly utilized to understand local polymer dynamics in the melt[4–9]. The trajectories from such simulations can be analysed in much greater detail than any set of experiments in order to build a picture of the mechanism of local polymer dynamics. Eventually this technique may allow a detailed understanding of how molecular structure determines T_g.

We report here molecular dynamics simulations of polyisoprene melts. Polyisoprene is an interesting choice for a number of reasons. First, polyisoprene is an important industrial polymer. Because of this, there is a large body of experimental data on both melt[10–14] and dilute solution[15,16] available for comparison with the simulations. Secondly, the structure of polyisoprene is more complex than that of the polymers previously investigated in this type of simulation. We would like to understand how this complexity affects the local dynamics. Thirdly, at the temperatures we have simulated (about 200 K above T_g), the local dynamics of polyisoprene are fast enough that meaningful information can be obtained during the nanosecond time window available in molecular dynamics simulations. Fourthly, we have recently reported a simulation of polyisoprene in dilute toluene solution[17]. For the first time, a detailed comparison can be made between simulated dynamics in solution and the melt. Some aspects of this comparison will be described in a future publication[18].

The local dynamics observed in these simulations are reasonably realistic as judged by comparison with n.m.r. experiments. The ratios of correlation times for different C–H vectors in the chain backbone match experiment very well. Absolute C–H vector correlation times from the simulation are about 2.5 times slower than experimental values. The shapes of the correlation functions calculated from the simulation are consistent with features inferred from experiment. Librational motions that occur on the scale of a few picoseconds play a significant role in the decay of the autocorrelation functions for C–H vectors.

Several interesting aspects of the local dynamics of polyisoprene melts are revealed by these simulations. The local dynamics in these simulations are fairly isotropic, in marked contrast to a recent simulation of polyethylene melts by Takeuchi and Roe[4]. The portion of the chain that rearranges cooperatively in order to localize a conformational transition is quite small, about 1–2 repeat units. Most conformational transitions occur cooperatively with other conformational transitions, but no single type of cooperative transition pair is particularly significant.

* To whom correspondence should be addressed

SIMULATION DESCRIPTION

We present results obtained from four molecular dynamics trajectories of bulk polyisoprene starting from independent initial configurations. Each cell consisted of a 100-mer of polyisoprene with cubic periodic boundary conditions. The polyisoprene used was 100% *cis*-1,4- and had all head-to-tail linkages. Its structure is shown below:

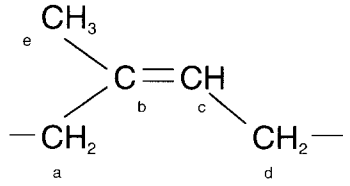

Experiments show that T_g for *cis*-1,4-polyisoprene has reached the high-molecular-weight limit for molecular weights greater than 3000 g mol^{-1} (ref. 19). Since the molecular weight of the simulated chain is 6800 g mol^{-1}, we expect that the local dynamics of the simulated chain are representative of those of a high-molecular-weight sample.

The molecular dynamics simulations were performed using Biosym's *Amorphous Cell* and *Discover* programs (Biosym Technologies Inc., San Diego, CA, USA). A 1 fs time step was used and the non-bonded potential energies were truncated after 8 Å. A nanosecond trajectory on a cell of 1302 atoms took about 15 days of CPU time on an IBM RS6000/325. The *NPT* ensemble (constant particle number, pressure and temperature) was used during the production portion of the runs at atmospheric pressure (after correction for the potential cutoff) and 413 K. We used Biosym's fully atomistic CFF91 force field[20,21]. The same force field was also used for recently reported simulations of polyisoprene in toluene[17]; the results from the melt simulations are compared to these solution simulations at several points in this paper.

A trajectory of a few nanoseconds is not nearly long enough to allow the polymer to fully explore phase space. Thus the observed local dynamics may be influenced by the initial configuration. We used four different initial configurations to test this. In addition, we used two very different methods to generate the initial configurations. As shown below, no important differences were observed among the four trajectories.

Generation at bulk density (runs 1 and 2)

Biosym's *Amorphous Cell* was used to build two cells at bulk density (estimated to be 0.836 g cm^{-3} at 413 K). This program uses a method developed by Theodorou and Suter[22] with modifications based on work by Meirovitch[23]. The backbone of the polymer is grown bond by bond sequentially. At each step, checks are made to assure that no overlap occurs with existing atoms. These cells were equilibrated using a procedure similar to that used by Li and Mattice[24]. Steepest-descents minimization (500 steps) was first used on the configurations generated by *Amorphous Cell*. Constant-volume molecular dynamics was then run for 10 ps, the first portion of which was used to heat the system to 1000 K at a rate of 100 K/100 fs. Twenty snapshots of the cell were saved from the last 5 ps. The snapshot with the lowest potential energy was then minimized using steepest descents (50 000 steps). The cell energies at this point were −1045 and −1010 kcal mol^{-1} for runs 1 and 2, respectively.

Generation in vacuum (runs 3 and 4)

The method of Kikuchi *et al.*[25] was used to generate two other initial configurations. Polymer chains were generated in vacuum (without periodic boundary conditions) and then slowly compressed to bulk density. The initial configurations had random torsional angles and were first subjected to 500 steps of steepest-descents minimization. Next, the polymers were heated to 1000 K as described above and afterwards cooled to 413 K. Cubic periodic boundary conditions were then applied with very large cell dimensions (about 150 Å on a side). Constant-pressure molecular dynamics was performed for about 200 ps, initially at 130 atm (uncorrected for potential truncation). The pressure was increased by 100 atm every 8 ps until the density of the system reached 0.836 g cm^{-3}. Fifty-thousand steps of steepest-descents minimization were finally performed, mainly in order to compare these configurations with those of runs 1 and 2. The final cell energies were −1120 and −1105 kcal mol^{-1} for runs 3 and 4, respectively, or within 0.11 kT per atom of runs 1–2 at 413 K.

Continuation of trajectories

Since the partially minimized structures of runs 1–4 all had similar energies, long molecular dynamics trajectories were performed starting from each. Constant-pressure (1 atm, corrected for potential truncation; the pressure was set much higher for the first 100 ps) and constant-temperature (413 K) molecular dynamics was run for 1500 ps. The positions of all the atoms were saved every 0.1 ps during the last 900 ps of the run. The densities displayed no systematic trends over these intervals. The densities, radii of gyration $\langle r_g^2 \rangle^{0.5}$ and the end-to-end distances $\langle r^2 \rangle^{0.5}$ for the four runs are shown in *Table 1*. The simulation densities are about 7% too low, indicating that the non-bonded terms in the force field are not perfectly calibrated. The chain dimensions vary but are always too small, probably as a result of the generation methods. The local dynamics of the four runs are quite similar (see below), indicating that chain dimension is not a critical parameter for this study.

Torsion populations

The polyisoprene backbone has three different types of carbon–carbon single bonds per repeat unit. We refer to these three torsions as ab, cd and da (see structure above). *Figure 1* shows symmetrized population distributions for these three torsions averaged over runs 1–4. The effective potentials (a potential of mean force) for each of the torsions can be inferred from the figure using the

Table 1 Density and chain dimensions[a]

	$\langle \rho \rangle$ (g cm^{-3})	$\langle r^2 \rangle^{0.5}$ (Å)	$\langle r_g^2 \rangle^{0.5}$ (Å)
Run 1	0.778 (0.011)	54 (3)	20 (0.2)
Run 2	0.774 (0.012)	48 (3)	19 (0.3)
Run 3	0.775 (0.012)	44 (3)	16 (0.2)
Run 4	0.772 (0.013)	39 (3)	13 (0.2)
Experiment	0.836	64	27

[a] Parentheses indicate standard deviations

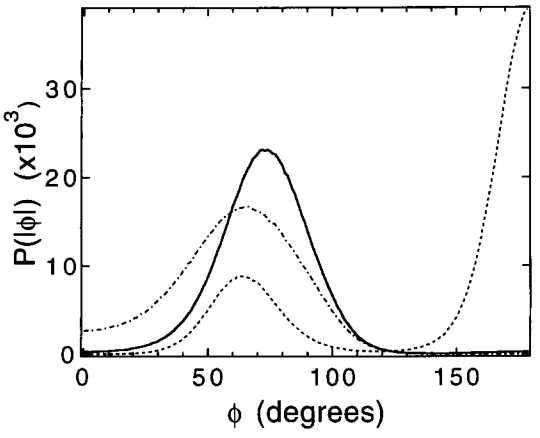

Figure 1 Symmetrized population distributions for torsions ab (——), cd (— · —) and da (– – – –)

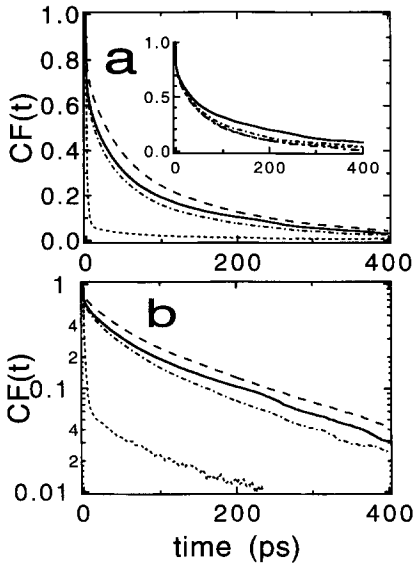

Figure 2 (a) P_2 orientation autocorrelation functions for polyisoprene C–H vectors a (——), c (— — —), d (— · —) and e (– – – –) averaged over runs 1–4. The inset shows the autocorrelation functions for C–H vector c from runs 1–4. Symbols are: run 1 (——), run 2 (— · —), run 3 (– – – –), run 4 (— — —). (b) Semi-logarithmic plot of correlation functions (averaged over runs 1–4). C–H vectors are specified by the carbon atom label in the structure given in the text. The presence of a very fast component and a non-exponential long-time decay are consistent with n.m.r. experiments

relationship $\ln P(\phi) = -E(\phi)/RT$. The effective potential for torsion da has three wells, while torsions ab and cd are two-fold, torsion cd being more 'loose' (i.e. lower barrier). Definitions of ϕ for the various torsions are as follows: $\phi = 0°$ for torsions ab and cd was defined to place all the carbon atoms in the same plane, as in the structure above; for torsion da, the *trans* state was defined to be $\phi = 180°$. The population distributions are very similar to those determined from our earlier simulation of a dilute polyisoprene/toluene solution[17]. The populations used to construct *Figure 1* were not quite symmetric, presumably due to the finite simulation time.

COMPARISON WITH N.M.R. EXPERIMENTS

In this section we compare the local dynamics of our simulated polyisoprene melt to experimental results. These comparisons indicate that the simulations qualitatively reproduce several important experimental results and quantitatively have correlation times within a factor of 2.5 of experimental values. The microscopic picture of local dynamics that emerges from these simulations is discussed in the next section.

N.m.r. measurements of local polymer dynamics

The T_1 values and NOEs (nuclear Overhauser enhancements) measured by ^{13}C n.m.r. are sensitive to the reorientation of C–H bonds in polymers. The experimental observables depend on the P_2 orientation autocorrelation function $CF(t)$ for C–H bond vectors:

$$CF(t) = \langle P_2(\hat{x}(0) \cdot \hat{x}(t)) \rangle = \langle 3 \cos^2 \theta(t) - 1 \rangle / 2 \quad (1)$$

Here P_2 is the second Legendre polynomial, $\hat{x}(t)$ is a unit vector in the direction of a particular C–H bond vector at time t, and $\theta(t)$ is the change in the vector orientation between time t and time 0. *Figure 2a* shows the correlation functions for the four different C–H bond vectors in polyisoprene averaged over runs 1–4. The three backbone C–H bond vectors reorient on roughly the same timescale while the methyl C–H reorients much more rapidly owing to nearly free rotation about the C_b–C_e bond. The inset to *Figure 2a* shows $CF(t)$ for C–H bond vector c for runs 1–4 individually and gives an indication of the similarity of the different runs. The five repeat units at each end of the chain were excluded from all calculations.

In the extreme narrowing regime, T_1 is independent of Larmor frequency and there is a direct relationship between T_1 and the time integral of $CF(t)$:

$$1/T_1 = 10nK\tau_c \quad (2)$$

Here K is a coupling constant, which depends on the bond length, and n is the number of protons bonded to the ^{13}C. The correlation time τ_c is defined as:

$$\tau_c = \int_0^\infty CF(t)\,dt \quad (3)$$

Note that, in the extreme narrowing regime, equations (2) and (3) are exact and independent of any assumed model of C–H vector motion.

^{13}C n.m.r. T_1 and NOE measurements for various backbone C–H vectors in bulk polyisoprene have been reported by Dejean de la Batie *et al.*[10] (92% *cis*) and Denault and Prud'homme[11] (71% *cis*) as a function of temperature. As our simulated polyisoprene was 100% *cis*, we will compare our simulations with ref. 10 for the three backbone C–H vectors. Since only ref. 11 reports results for the methyl C–H vector, these experiments will be used in this case.

Absolute correlation times

At the highest temperature reported in refs 10 and 11 (370 K), T_1 is not yet independent of Larmor frequency. However, an extrapolation of these data to the simulation temperature (413 K) indicates that the extreme narrowing condition would probably hold. Equation (2) was used to determine the experimental τ_c values from extrapolated T_1 values. We estimate that this extrapolation introduces an error of 25% or less.

Table 2 Polyisoprene correlation times (ps)[a]

C–H vector	Run 1	Run 2	Run 3	Run 4	Simulation average	Experiment[b]
a	75	53	62	51	60	26[c]
c	95	66	75	63	75	35[c]
d	62	45	50	44	50	22[c]
e	9.4	7.7	7.3	7.1	7.6	3.6[d]

[a] The values reported do not include correlation function tails (see text)
[b] Extrapolated from lower temperature; accuracy estimated to be 25%
[c] Ref. 10
[d] Ref. 11

Correlation times were calculated from individual simulation runs by numerically integrating the correlation functions from $t = 0$ to 400 ps. These values are found in *Table 2* for runs 1–4 along with the correlation times extrapolated from experimental measurements at lower temperatures. (A more detailed discussion of the comparison between τ_c values from n.m.r. and simulations is given in ref. 17.) The simulated correlation times are about a factor of 2.5 slower than the experimental values. However, the right trends are predicted: C–H vector e is faster than d is faster than a is faster than c. In addition, the ratios of the different correlation times match experiment very well.

As can be seen in *Figure 2a*, the correlation functions calculated from the simulation do not decay completely to zero by 400 ps. Thus the numerical integration of these curves as described above underestimates τ_c. We used several curve-fitting schemes in order to estimate the additional area of the functions beyond 400 ps. These methods all indicated that the missing area was likely to be small, about 10% for the backbone C–H and 20% for the methyl C–H. Thus we regard the simulation correlation times reported in *Table 2* as reasonable estimates but lower bounds.

Most bulk polymer simulations have not been tested against experiments that are sensitive to the local polymer dynamics. The present simulations are in closer agreement with n.m.r. results than any others of which we are aware. Comparison with n.m.r. was also made in a recent simulation of *cis*-polybutadiene[5], where the simulated dynamics were found to be a factor of 15 times too slow. (Agreement within a factor of 1.5 was reported in ref. 5, but a factor of 10 was omitted from equation (16) of that publication.)

Correlation function shapes

Outside of the extreme narrowing regime, ^{13}C n.m.r. T_1 and NOE measurements are sensitive to the shape of the C–H vector orientation autocorrelation function. The correlation functions for our melt simulations are shown in semi-logarithmic format in *Figure 2b*. These functions indicate that C–H bond vectors lose their orientation on two well separated timescales; the long part of the simulated correlation functions are strongly non-exponential (a straight line would indicate a single exponential). Dejean de la Batie *et al.*[10] interpreted their n.m.r. results using a correlation function shape that is qualitatively consistent with these observations. (We also tried to fit these data using our simulated correlation functions and the assumption that the correlation function shapes were temperature-independent. We did not achieve good agreement. Thus, either this assumption or the simulated correlation function shapes are incorrect.) Thus the simulation results support the position of ref. 10 regarding the existence of a very fast initial drop in $CF(t)$; this interpretation has recently been questioned by Rossler and Eiermann[26]. In contrast to the melt behaviour, experiment[15] and simulations[17] on polyisoprene in solution indicate that the long part of the correlation function decay is nearly exponential. Thus the mechanism of C–H vector reorientation is probably more complex in the melt than in solution.

MICROSCOPIC VIEW OF LOCAL POLYMER DYNAMICS

In this section we discuss the results of a number of different analyses of the mechanism of local polymer motion. The main issues addressed are the anisotropy of segmental motion and the length scale of cooperative motions. The comparison between simulation and experiment in the previous section indicates that the simulations are reasonably realistic. Thus we believe it is likely that the qualitative features discussed in this section are also reasonably realistic.

Motion in a pipe?

Takeuchi and Roe[4] analysed molecular dynamics simulations of polyethylene melts in terms of the anisotropy of local polymer dynamics. They calculated orientation autocorrelation functions for various vectors fixed in the molecular frame and found that a vector parallel to the chain backbone reoriented much more slowly than did a perpendicular vector. Takeuchi and Roe showed that this effect remained even in the absence of the torsional potential and that it was due to the dense packing of the chains in the melt. They envisioned that motion occurs within a rigid 'pipe' where a polyethylene molecule can rotate much more rapidly about its long axis than in any other direction.

We were curious to see if polyisoprene in the melt would display the same motional anisotropy as polyethylene. We calculated P_1 and P_2 orientation autocorrelation functions for vectors parallel and perpendicular to the polyisoprene backbone. The P_2 correlation function is defined by equation (1); the P_1 function is $\langle \cos\theta(t) \rangle$. The perpendicular vectors were defined relative to the planes containing three consecutive carbons along the chain backbone. The parallel vectors were defined by connecting second-neighbour backbone carbon atoms (a to c, b to d, c to a, d to b). In each case we averaged over the four different vectors per

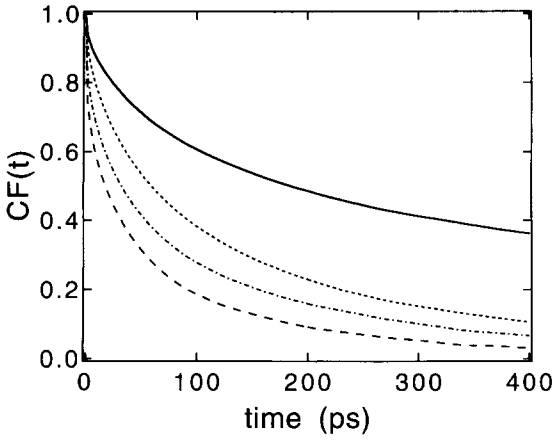

Figure 3 Orientation autocorrelation functions for vectors parallel (P_1 (———), P_2 (— · —)) and perpendicular (P_1 (– – – –), P_2 (— — —)) to the chain axis. Local dynamics in polyisoprene melts are much more isotropic than in polyethylene melts[4]

Table 3 Values of 1/e relaxation times (ps) for vectors parallel and perpendicular to the chain axis

	Polyisoprene (413 K)	Polyethylene (443 K)[a]
$P_1(\parallel)$	387	588
$P_2(\parallel)$	63	8.7
$P_1(\perp)$	107	2.7
$P_2(\perp)$	38	0.94
$P_1(\parallel)/P_1(\perp)$	3.6	218
$P_2(\parallel)/P_2(\perp)$	1.7	9.3

[a] Ref. 4

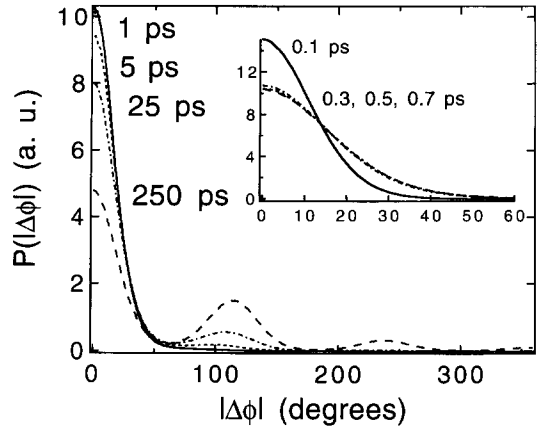

Figure 4 Probability of angular change $|\Delta\phi|$ for three-fold torsion da at various time intervals. The inset shows shorter time intervals. Librational motions in the bottom of potential wells equilibrate in about 0.3 ps, while conformation transitions occur at much longer times

repeat unit. The five repeat units at each end of the chain were excluded from the calculations.

The autocorrelation functions for parallel and perpendicular vectors in polyisoprene are shown in *Figure 3*. Following Takeuchi and Roe, we define the relaxation time to be the time required for the function to decay to 1/e. *Table 3* compares the relaxation times for parallel and perpendicular vectors in polyisoprene to those reported for polyethylene in ref. 4. Although the absolute relaxation times are difficult to compare, the ratios of relaxation times for parallel and perpendicular vectors are much closer to unity for polyisoprene melts than for polyethylene melts. Thus the local dynamics of polyisoprene are much more isotropic than those of polyethylene, despite the fact that both systems consist of densely packed hydrocarbon chains.

The less regular structure of polyisoprene is probably responsible for the more isotropic local motion observed in the polyisoprene simulations. Because of its methyl groups, polyisoprene does not fit into a 'pipe' as well as polyethylene. Surrounding chains are not so likely to form a 'pipe', as the torsional potentials in polyisoprene disfavour linear conformations. It is also possible that the united-atom approximation used in ref. 4 accentuates the regularity of polyethylene.

Regardless of the exact physical description, it would appear that the anisotropy of local motion in polymer melts can be influenced both by chain packing and by polymer structure (possibly including torsional potentials). We suspect that most amorphous polymers would not behave similarly to polyethylene because of their more complex repeat-unit structure. We also suspect that polyethylene in a different condensed-phase medium, such as a dilute solution, would not display the pronounced motional anisotropy of polyethylene in the melt.

Time evolution of torsional coordinates

Figure 4 shows the probability P of observing an angular change $|\Delta\phi|$ during various time intervals for the three-fold torsion da[27]. As shown in the inset, many torsions have already adjusted by 10–30° within 0.3 ps. This feature of the torsional angle distribution changes little as time evolves. At much longer times, new peaks centred at 120° and 240° grow in, indicating transitions to other conformational states. Fast motions within potential wells reach their equilibrium distribution before a significant number of conformational transitions occur.

Conformational transitions

Polyisoprene has three different torsions per repeat unit and the conformational transitions (defined as in ref. 17) of each had distinct characteristics in our simulation. We counted 12 125 total conformational transitions on the central 90 repeat units during the combined 3.6 ns of the four runs. (The number of conformational transitions varied by no more than 7% among runs 1–4.) Of this total, 28% occurred at an ab torsion, 42% at a cd torsion and 30% at a da torsion compared to 17%, 44% and 39% in solution[17]. The average time between transitions is about 35% shorter in the melt than in solution; this is probably a result of the higher temperature of the melt simulation (413 K vs. 298 K). It is surprising given this result that the correlation times for C–H bond vector reorientation are about 4 times longer in the melt than in solution. These observations question the existence of a direct connection between conformational transitions and the reorientation of C–H vectors, and will be discussed elsewhere[18].

We did not observe the pronounced spatial heterogeneity of conformational transitions that was observed in the polyisoprene solution simulations[17]. The difference in temperature for the two simulations may again be responsible for this. A quantitative calculation of the spatial heterogeneity of conformational transitions in the melt simulations was carried out following the example

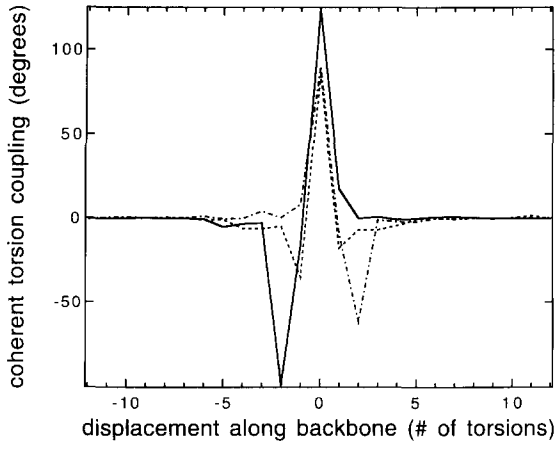

Figure 5 Change in torsional angles accompanying a conformational transition at position 0 (equation (4), $\Delta t = 0.5$ ps). The three different torsions of polyisoprene are labelled as in *Figure 1*. Most of the torsional adjustments occur within one repeat unit of the transforming bond. The double bond (torsion bc) is not included in this analysis

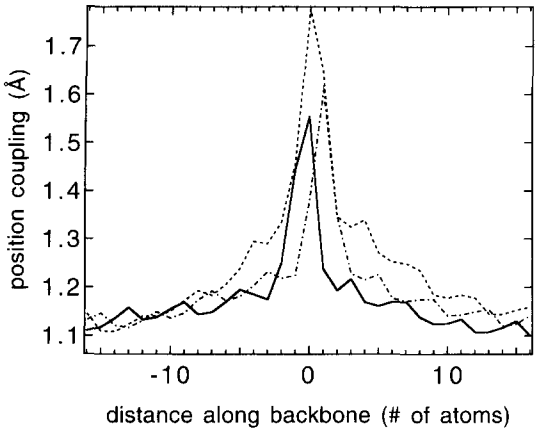

Figure 6 Distortion of atomic coordinates accompanying a conformational transition for the three torsions of polyisoprene (equation (5), $\Delta t = 0.5$ ps). Labelling scheme is the same as in *Figure 1*. The triggering conformational transition occurs between atoms 0 and 1. The region of enhanced distortion is largely limited to two repeat units

of Gee and Boyd[6]. We found heterogeneity comparable to that reported in ref. 6 for *cis*-polybutadiene at 400 K.

Torsion and position coupling analysis of conformational transitions

Conformational transitions in a polymer backbone are not completely isolated events[28,29]. Other degrees of freedom play a major role in localizing and thereby facilitating conformational transitions. We are interested in the spatial extent of this localization. How large is the cooperatively rearranging region along the polymer backbone?

The degree to which conformational transitions are localized in polyisoprene melts can be illustrated using two calculations[17,27]. Conceptually, we take snapshots of the atoms nearby a conformational transition just before and after the transition occurs (at time τ_{trans}). We can then ask what changed in the time interval ($2\Delta t$) between the two snapshots. One calculation examines how neighbouring torsions change as a function of distance along the chain. A second calculation examines how far carbon atoms in the chain backbone move during this time interval. We average over all transitions of a given type (ab, cd, or da) that occur in a trajectory and also over runs 1–4.

Figure 5 shows the average angular displacement of a torsional coordinate ϕ *in the same direction* as a triggering conformational transition:

$$\langle A(\Delta\phi)|\phi(\tau_{trans} + \Delta t) - \phi(\tau_{trans} - \Delta t)|\rangle \qquad (4)$$

Here $A(\Delta\phi)$ is chosen to be ± 1 to accomplish this. For example, if a torsion rotates in the same direction as the triggering transition, it counts positively to the average; if it rotates in the opposite sense, it counts negatively. Position 0 on the abscissa is defined by the conformational transition, and positive and negative values represent neighbouring torsions to the right and left along the chain. For example, looking at torsion ab in *Figure 5*, position -1 is a da torsion, $+1$ is a cd torsion, -2 is a cd torsion, etc. Note that the double bond (torsion bc) is not included in this analysis. The maximum angular distortion is found at position 0 in each case. Far away on either side of position 0, the baseline goes to zero as torsions far away from the triggering transition are equally likely to rotate in either sense.

Figure 5 indicates that the region of cooperative motion associated with a conformational transition is largely limited to 3–4 torsions, or about one repeat unit. (Calculation of absolute torsion coupling, as in *Figure 5* in ref. 17, indicates a similar length scale of cooperativity). Similar results were obtained for polyisoprene in dilute toluene solution[17]. The large secondary peaks in *Figure 5* (at position -1 for torsion da, $+2$ for torsion cd, and especially position -2 for torsion ab) indicate the torsional motion most strongly coupled to the conformational transition. These peaks are negative and represent crank-like counter-rotation, which predominates over co-rotation. As noted in ref. 17, the location of these peaks indicates that most cooperative motion in polyisoprene takes place in the flexible region in between the double bonds; the $-CH{=}C{-}CH_3-$ groups seem to act as rigid anchor points. It is important to emphasize that many of the adjustments that neighbouring torsions make in order to accommodate a conformational transition do not involve a second conformational transition. *Figure 4* illustrates that relatively large-amplitude torsional motion can occur quite rapidly within a potential well.

Figure 6 shows the average changes in atomic positions accompanying a conformational transition:

$$\langle |\boldsymbol{r}(\tau_{trans} + \Delta t) - \boldsymbol{r}(\tau_{trans} - \Delta t)|\rangle \qquad (5)$$

The site of the triggering transition defines backbone atoms 0 and 1 on the abscissa. For example, for torsion ab, position 0 is atom a, position 1 is atom b, position 2 is atom c, etc. We see maximum displacement at position 0 or 1. Most of the excess displacement associated with the conformational transition seems to be localized to two repeat units (four backbone carbon atoms per repeat unit).

The major differences between the results of the polyisoprene melt and solution simulations are as follows. Conformational transitions at torsion cd require more compensating motion from a neighbouring ab torsion in the melt (position $+2$ in *Figure 5*). The position coupling plot (*Figure 6*) may show some cooperativity on

a longer length scale in the melt than in solution; this comparison is ambiguous because the solution results are quite noisy. Overall the cooperativity of conformational transitions in polyisoprene appears to be quite similar between melt and solution. We have recently carried out simulations of an isolated polyisoprene chain in vacuum, which confirmed the observation that the cooperativity associated with conformational transitions in polyisoprene is relatively insensitive to the chain environment[18].

In addition to considering motion along the chain backbone that occurs in conjunction with a conformational transition, we have also looked for motion in segments that are close in space but far away along the chain contour. Very little of this 'intermolecular' cooperativity was found. In retrospect, this is not surprising considering the narrow region of cooperativity along the chain. Non-bonded segments adjacent to a segment undergoing a conformational transition are at least 4–5 Å away, or about the length of one repeat unit. Little cooperativity is seen along the chain at these distances and so it is reasonable that little is seen in neighbouring non-bonded segments.

Cooperative transition pairs

Often cooperativity in conformational transitions has been discussed in terms of cooperative transition pairs[17,27,30–33]. This viewpoint emphasizes the role that nearby conformational transitions can play in localizing each other. As such, it complements the more general coupling analysis discussed above.

We analysed the cooperative transition pairs in our simulation using the method described in ref. 17. Conceptually, we want to look far enough away from a triggering transition in both space and time to include all other transitions with which it might be correlated. However, when a large space and time window is considered, many transitions that occur in that window are random events, i.e. not correlated with the triggering transition. The cooperative events are those which occur in excess of random probabilities. The most difficult aspect of the calculation is accounting for the random events so that they can be subtracted from the total. (The method used in this calculation is the one which generated a lower bound to the fraction of random events in ref. 17.)

Figure 7 shows the probability of finding a cooperative conformational transition as a function of the absolute value of the distance along the chain between the triggering transition and the cooperative transition; random events have been subtracted. For simplicity, we have averaged over the three types of torsions and in both directions along the chain. The different curves correspond to different time cutoffs for cooperativity; a second transition was considered as potentially cooperative if it occurred in a time window $\pm\Delta t$ relative to the triggering transition. Second-neighbour cooperative transition pairs occur with the greatest probability. This is consistent with the strong coupling between torsions ab and cd seen in *Figure 5*. As one looks far along the chain from a triggering transition, the probability of a cooperative event goes to zero. Substantial coupling is seen out to about third or fourth neighbours, yielding a length scale of cooperativity of perhaps two repeat units, which is consistent with the previous analysis.

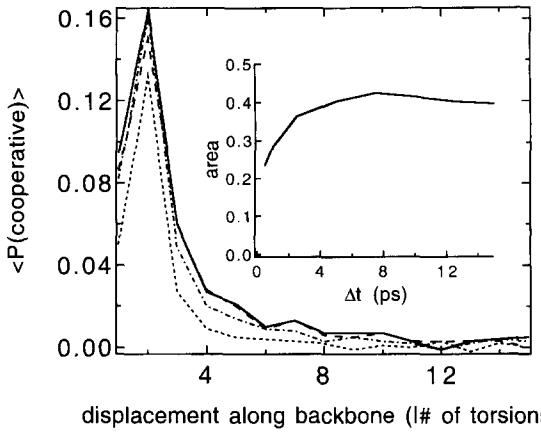

Figure 7 Probability of cooperative conformational transitions (after subtracting random events) found to occur in neighbouring torsions, averaged over all three types of torsions and in both chain directions. Values of Δt are 0.5 ps (– – – –), 2.5 ps (— · —), 7.5 ps (——), 15 ps (— —). Cooperative transitions occur with reasonable probability out to about fourth neighbours. The inset shows the area under these curves plotted vs. Δt. Cooperative events stop accumulating after about 7.5 ps. The double bond (torsion bc) is not included in this analysis

Table 4 Fraction of polyisoprene conformational transitions cooperative with at least one other transition

Cumulative fraction through	Melt (413 K)	Dilute toluene solution (298 K)[a]
First neighbours	0.20	0.15
Second neighbours	0.50	0.36
Fourth neighbours	0.60	0.55
Sixth neighbours	0.63	0.60
Eighth neighbours	0.65	0.65
Tenth neighbours	0.67	0.67

[a] Ref. 17

Table 4 shows the fraction of conformational transitions that occur in cooperation with at least one other transition. The values in *Table 4* were calculated using a time window of 7.5 ps[17]; the inset to *Figure 7* shows that the area under the curves in the main figure becomes constant by this time. *Table 4* indicates that there are more cooperative events between first through third neighbours in the melt simulations than were found previously in polyisoprene solution simulations. This is consistent with the torsion and position coupling analysis above. Cooperative transition events extend over a longer length scale in solution. This is apparently inconsistent with the results of the torsion and position coupling analysis.

We repeated this analysis allowing a back-transition at a given torsion to count as a cooperative event. More than half of all conformational transitions in the melt occur nearby in time to another transition on the same torsion (after correcting for random events). These back-transition events were somewhat less prominent in the solution simulations, happening about one-third of the time.

Apart from back-transitions, no single type of conformational transition pair occurred with great frequency. The most common was an ab torsion cooperating with a cd torsion to its left (see structure above); this occurred for 35% of the conformational transitions at torsion ab. This type of cooperative event

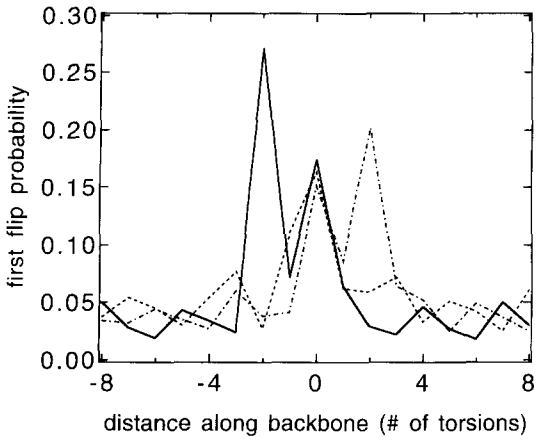

Figure 8 Spatial location along chain of the first conformational transition that follows a triggering transition at position 0. The labelling scheme for the three torsions of polyisoprene is given in *Figure 1*. The region of cooperative transitions is 1–2 repeat units. The double bond (torsion bc) is not included in this analysis

involved only about 20% of all conformational transitions observed in the trajectories. No other type of cooperative transition pair accounted for more than a few per cent of the events observed.

First-failure pair analysis

Gee and Boyd[6] recently developed a method for analysing cooperative transition pairs based on a first-failure analysis. After a conformational transition occurs at some location, the next transition to occur on a nearby torsion $\pm i$ away is binned at $\pm i$ and a histogram of first-failure pairs is built up. We performed this analysis on our trajectories, partly in order to see how various methods of analysing cooperativity would compare.

The results of the first-failure analysis on conformational transitions in polyisoprene melts are shown in *Figure 8*. About 15–20% of the time the next conformational transition to occur in the range $\pm i$ occurs at the same site as the triggering transition. Many conformational transitions at an ab torsion are next followed by a transition at a cd torsion (position −2); many conformational transitions at torsion cd are followed by another at torsion ab (position +2). Qualitatively, these features are also seen in the torsion coupling plot (*Figure 5*). The baseline is rapidly approached as conformational transitions far away from the trigger at position 0 become uncorrelated. The region of cooperativity is about 1–2 repeat units. These results are in general agreement with the previous analyses of cooperative motion.

CONCLUDING REMARKS

The simulations of polyisoprene melts reported here, and those previously reported for a dilute polyisoprene/toluene solution[17], compare favourably with experiments sensitive to local polymer dynamics. Thus we expect that the qualitative features of local polymer dynamics extracted from an analysis of the simulations are reasonably realistic. In both solution and the melt, orientation autocorrelation functions for C–H vectors have very fast initial decays, which can be attributed to librational motion in torsional potential wells. The major portion of the correlation function decays are nearly exponential in solution but strongly non-exponential in the melt, indicating a more complex relaxation mechanism in the melt.

Local dynamics in polyisoprene melts are much more isotropic than those in the polyethylene melts simulated by Takeuchi and Roe[4]. This is probably due to local ordering among polyethylene chains, which is not present to the same extent in polyisoprene. The more regular repeat-unit structure of polyethylene facilitates this ordering. We suspect that the more isotropic dynamics observed for polyisoprene melts is typical of most amorphous polymers.

Several methods of analysis indicate that the cooperative motions that help to localize conformational transitions in polyisoprene are limited to a region of 1–2 repeat units. This may be related to polyisoprene's low T_g (200 K). Polymers with higher T_g may have a larger length scale of cooperativity[34].

An analysis of cooperative events involving multiple conformational transitions indicates that most conformational transitions in polyisoprene melts are associated with such events. However, many different types of such events were found and no one type (except for back-transitions) accounts for a substantial fraction of all events. Thus, no simple picture involving only rotational isomeric states can represent cooperativity in polyisoprene. Our simulations suggest a very heterogeneous picture where the displacements of neighbouring torsions are more usefully viewed as a continuous process.

The cooperativity of conformational transitions in polyisoprene is surprisingly similar in the melt and in solution. The melt environment somewhat increases the probability of a second conformational transition very near an initial transition. In addition, a larger fraction of conformational transitions in the melt are back-transitions. These observations are consistent with some recent simulations of phantom chains and chains in the bulk[6,35].

An interesting difference between the solution and melt simulations involves the relationship between C–H vector correlation times and the average times between conformational transitions. In the melt these two times are quite similar, while they are significantly different in solution. This observation questions the common assumption that conformational transitions are primarily responsible for the decay of the C–H vector correlation functions and will be investigated further[18].

ACKNOWLEDGEMENTS

This work was supported by the National Science Foundation (DMR-9424472). The computers used in this work were purchased through a grant from the NSF Chemistry Division (CHE-9007850).

REFERENCES

1 Aklonis, J. J. and MacKnight, W.J. 'Introduction to Polymer Viscoelasticity', Wiley, New York, 1983, Ch. 4
2 Pschorn, U., Rössler, E., Sillescu, H., Kaufmann, S., Schaefer, D. and Spiess, H.W. *Macromolecules* 1991, **24**, 389.
3 Schaefer, D., Spiess, H. W., Suter, U. W. and Fleming, W. W. *Macromolecules* 1990, **23**, 3431
4 Takeuchi, H. and Roe, R.-J. *J. Chem. Phys.* 1991, **94**, 7446
5 Kim, E.-G. and Mattice, W. L. *J. Chem. Phys.* 1994, **101**, 6242
6 Gee, R. H. and Boyd, R. H. *J. Chem. Phys.* 1994, **101**, 8028

7 Roe, R.-J. *J. Chem. Phys.* 1994, **100**, 1610
8 Kikuchi, H., Tokumitsu, H. and Seki, K. *Macromolecules* 1993, **26**, 7326
9 Smith, G. D., Yoon, D. Y., Zhu, W. and Ediger, M. D. *Macromolecules* 1994, **27**, 5563
10 Dejean de la Batie, R., Lauprêtre, F. and Monnerie, L. *Macromolecules* 1989, **22**, 122
11 Denault, J. and Prud'homme, J. *Macromolecules* 1989, **22**, 1307
12 English, A. D. *Macromolecules* 1985, **18**, 178
13 Schaefer, J. *Macromolecules* 1973, **6**, 882
14 Zorn, R., Richter, D., Farago, B., Frick, B., Kremer, F., Kirst, U. and Fetters, L. J. *Physica (B)* 1992, **180/181**, 534
15 Gisser, D. J., Glowinkowski, S. and Ediger, M. D. *Macromolecules* 1991, **24**, 4270
16 Glowinkowski, S., Gisser, D. J. and Ediger, M. D. *Macromolecules* 1990, **23**, 3520
17 Moe, N. E. and Ediger, M. D. *Macromolecules* 1995, **28**, 2329
18 Moe, N. E. and Ediger, M. D. *Macromolecules* to be submitted
19 Widmaier, J. D. and Meyer, G. C. *Macromolecules* 1981, **14**, 450
20 Maple, J. R., Dinur, U. and Hagler, A. T. *Proc. Natl. Acad. Sci. USA* 1988, **85**, 5350
21 Maple, J. R., Thacher, T. S., Dinur, U. and Hagler, A. T. *Chem. Des. Automat. News* 1990 **5**(9), 5
22 Theodorou, D. N. and Suter, U. W. *Macromolecules* 1985, **18**, 1467
23 Meirovitch, H. J. *Chem. Phys.* 1983, **79**, 502
24 Li, Y. and Mattice, W. L. *Macromolecules* 1992, **25**, 4942
25 Kikuchi, H., Seke, K. and Kuwajima, S. *Macromolecules* submitted
26 Rossler, E. and Eiermann, P. *J. Chem. Phys.* 1994, **100**, 5237, 5245
27 Adolf, D. B. and Ediger, M. D. *Macromolecules* 1991, **24**, 5834
28 Schatzki, T. F. *J. Polym. Sci.* 1962, **57**, 496
29 Helfand, E. *Science* 1984, **226**, 647
30 Boyd, R. H., Gee, R. H. and Jin, H. *J. Chem. Phys.* 1994, **101**, 788
31 Zuniga, I., Bahar, I., Dodge, R. and Mattice, W. J. *J. Chem. Phys.* 1991, **95**, 5348
32 Helfand, E., Wasserman, Z. R. and Weber, T. A. *Macromolecules* 1980, **13**, 526
33 Baysal, C., Erman, B. and Bahar, I. *Macromolecules* 1994, **27**, 3650
34 Ediger, M. D. and Adolf, D. B. *Adv. Polym. Sci* 1994, **116**, 73
35 Smith, G. D., Yoon, D. Y. and Jaffe, R. L. *Macromolecules* 1995, **28**, 5897